J Appl Electrochem (2011) 41:405–413
DOI 10.1007/s10800-010-0250-3

ORIGINAL PAPER

Investigation of N_2-fixation on polyaniline electrodes in methanol by electrochemical impedance spectroscopy

Fatih Köleli · Derya Röpke · Rezzan Aydin · Thorsten Röpke

Received: 25 January 2010 / Accepted: 21 November 2010 / Published online: 14 December 2010

Abstract The ac response of polyaniline thin films on platinum electrodes was measured at different dc potentials during the N_2-fixation in methanol + $LiClO_4$ electrolyte with 0.03 mol L^{-1} H_2SO_4 for the first time. The optimum film thickness was found to be 1.5 μm, N_2-pressure 50 bar and an optimum electrolysis potential of −0.12 V (NHE). The diffusion coefficients for N_2 into the polymer film was found to be $(5 \pm 2)\times10^{-9}$ cm^2 s^{-1}.

Keywords Polyaniline · N_2-fixation · H_{ad} formation · Electrochemistry · Electrochemical impedance spectroscopy (EIS)

1 Introduction

Artificial dinitrogen fixation under mild conditions is a chemical challenge of great significance. Because, dinitrogen is a simple inert molecule whose great inertness is reflected in its high bond dissociation enthalpy (945 $kJmol^{-1}$), high ionisation potential (15.058 eV) and negative electron affinity (−1.8 eV). Examination of the N_2 molecular orbital diagram and the orbital energies reveal strongly bonding occupied orbitals (of energies −15.6, −17.1, −18.7 and −39.5 eV) with a very large energy gap (22.9 eV) between the highest occupied (HOMO) and lowest unoccupied (LUMO) molecular orbitals [1].

F. Köleli (✉) · D. Röpke · R. Aydin
Department of Chemistry, Mersin University,
33342 Mersin, Turkey
e-mail: fkoleli@mersin.edu.tr

T. Röpke
Hydrogen Institute of Applied Technologies gGmbH (HIAT),
Hagenower Straße 73, 19061 Schwerin, Germany

Generally, the enzymatic reactions need mild conditions compared to the Haber–Bosch process. With the aim of having mild conditions chemically, a large variety of investigations into the synthesis and reactivity of N_2-transition metal complexes were stimulated [2–6]. In all of these studies, ammonia concentrations were in the range of 1–20 μmol L^{-1}, and excitations by light was necessary. In an electrochemical study, dinitrogen was reduced at an extremely negative potential of −4.0 V (Ag|AgCl) on different metal electrodes in $LiClO_4$ + THF + EtOH electrolyte, where Li acts as a mediator [7]. In further study, electrochemical reduction of dinitrogen to ammonia was investigated on ruthenium electrode with a Faradaic efficiency of 0.0015% [8]. In other study, the synthesis of ammonia from nitrogen and water was investigated on Ru cathodes in Solid Polymer Electrolyte Cell at −1.02 V (Ag/AgCl) with 0.003% of the reaction chemical yield [9]. In further study, electrochemical conversion of N_2 to NH_3 was investigated at 60 °C and ambient pressure too reduced on C_{60} at −0.8 V (Ag/AgCl) [10].

To explore new electrode materials, conductive polymers provide a feasible alternative to well-known metals and metal alloys. However, investigations of conducting polymers at the cathodic side of the potential scale are rare. Polyaniline (PAn) was studied most intensively by EIS [11–20] to complement and elucidate current–voltage and mass transport characteristics at the positive side of the potential scale.

A PAn film modified with platinum microparticles as electrode material was investigated via EIS between −0.25 and −0.7 V (SCE) to achieve data of various charge transfer and transport processes involved in the electrochemical response of this polymer electrode [21]. EIS generally has an advantage—among other electrochemical methods—in systems having large disturbances; the

studied system is not far from the steady-state. This advantage is important, when we consider conducting polymer films which can show perturbations in a large potential window because of their inhomogeneous structure. We investigated the impedance spectroscopic behaviour of a PAn film by EIS at negative potentials in a previous work [22].

Previously, we also investigated the dinitrogen reduction on a PAn-coated platinum electrode at an extremely low overpotential of −0.12 V (NHE) in methanol + $LiClO_4$ as supporting electrolyte under pressure values of 1, 20, 40, 50, 60 and 80 bar and achieved ammonia concentrations up to 57 μmol L^{-1} with maximum Faradaic efficiency of 16% [23]. The aim of this study was to obtain the kinetic data and reaction mechanism of N_2-fixation on a PAn electrode under high pressure values through the impedance spectroscopy.

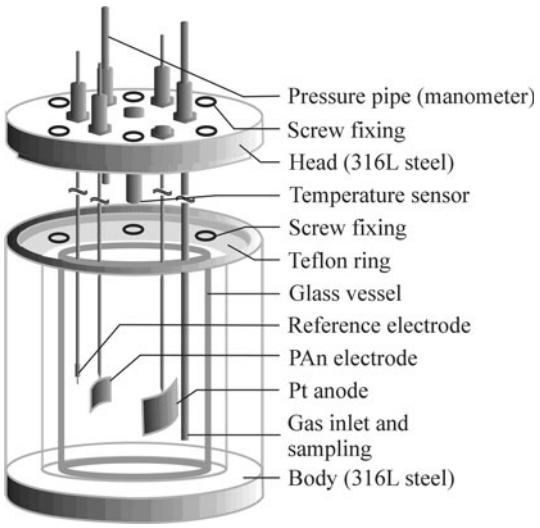

Fig. 1 High pressure cell used for electrolysis and EIS measurements. In electrolysis the Pan electrode had an area of 8 cm^2 (Pt anode 1 cm^2)

2 Experimental

Polyaniline was synthesized potentiodynamically from a stock solution of 0.1 mol L^{-1} freshly distilled aniline (Fluka) between −0.2 and +0.85 V (Ag|AgCl) on a Pt-plate (surface area of 1 cm^2) with a thickness of *ca.* 1.5 ± 0.2 μm (40 cycles; scan rate 50 mV s^{-1}) in 0.5 mol L^{-1} H_2SO_4. The counter electrode was a Pt-plate (8 cm^2) and throughout the measurements under ambient and higher pressure conditions, a $Pb(Hg)_x|PbSO_4|SO_4^{2-}$ electrode with a potential of −50 mV (NHE) was used as a reference electrode [1]. In order to remove the surplus ions and other impurities in the polymer film, the electrode was washed carefully with methanol and transferred into the high pressure cell used for the impedance measurements. The preparative electrolysis and the impedance measurements were carried out (CHI Electrochemical Work Station, Model 660A) in an undivided high pressure cell which was constructed from 316L stainless steel (Fig. 1). A glass vessel with *ca.* 80 cm^3 of volume having the same shape like steel mantle was placed into the cell for electrical isolation. In order to supply constant pressure within the cell, the electrodes were sealed and electrically isolated from the cell-body by Teflon fittings. Furthermore, the cell-head had a manometer to monitor internal pressure (Fig. 1).

The EIS measurements were carried out at 25 °C at different potentials in a frequency range from 100 kHz to 0.1 Hz (ac amplitude of 10 mV) in MeOH + 0.1 M $LiClO_4$. The inductance of the leads was measured and could be neglected (1 μH). As proton source, 1 mol L^{-1} H_2SO_4 in methanol (0.03 mol L^{-1}) was added into the electrolyte. Before each EIS measurement, the electrolyte was saturated with N_2. Some of the equivalent circuits proposed earlier [14, 16, 18–20] were used to fit the experimental data (software ZView 2.1b, developed by Scribner Associates Inc., USA). The fitting results were used for the calculation of the diffusion coefficient of dinitrogen in the polymer film.

3 Results and discussion

3.1 Generally

The EIS measurements were carried out systematically with respect to applied potential, film thickness and applied pressure to examine the general cathodic impedance characteristics of a PAn film during the N_2 reduction in the electrolyte. To understand the behaviour of a coated metal from the point of electrochemical impedance spectroscopic view, the metal/polymer/solution interface is presented schematically in Fig. 2.

After coating of a metal plate with a conducting polymer film, pores remain at the surface of supporting metal. A representative open pore in which the electrochemical reaction occurs, provide the contact to electrolyte (Fig. 2) and the diffusion of the electroactive substrate from the solution to the metal surface takes place in these open pores [24]. In that case, the double layer is placed between metal and the solution in this pore. The polymer film on the surface is charged during electrochemical polarization and can act as a capacitor. With this consideration, equivalent circuits can be proposed for calculation of the EIS curves (Nyquist curves). The Nyquist curves recorded during the EIS measurements were fitted by using equivalent circuits in Fig. 3. The circuit in Fig. 3a is commonly used one for

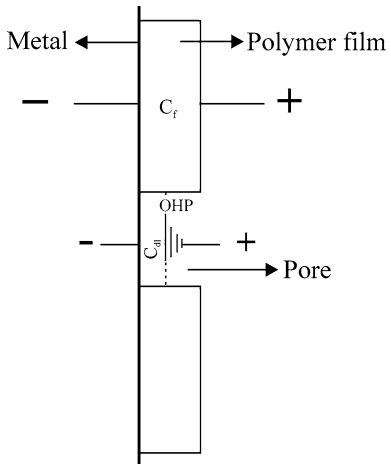

Fig. 2 Metal/polymer/solution interface, C_{dl} Double layer capacitance of metal/solution interface, C_f film capacitance, *OHP* outer Helmholtz plane [22]

coated metals and described well in the literature [24–32]. The second equivalent circuit in Fig. 3b has a Warburg impedance (Z_{FLW}) caused through diffusion of the intermediates which formed from N_2 hydrogenation. Furthermore, for comparasion of the curves, the ac impedance response of a PAn film depending on the applied potential is recorded and presented in Fig. 4.

3.2 Interpretation of the impedance spectra

The obtained Nyquist curves have two semicircles and a diffusion part at low frequencies. The first semi-circle at high frequencies may describe the metal/solution double layer (Fig. 2). This double layer can be characterized as the sum of the pore resistance R_1 and Constant Phase Element CPE_1 (metal/solution double layer capacity).

The impedance of a constant phase element Z_{CPE} is calculated by Eq. 1

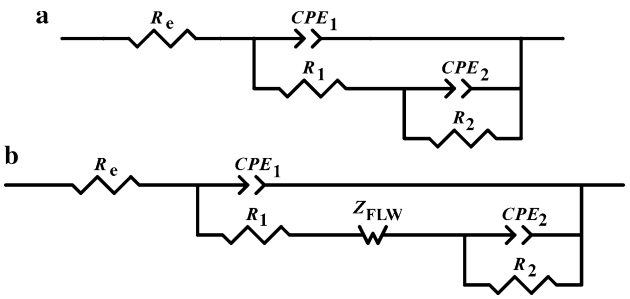

Fig. 3 Equivalent circuits for the PAn electrode **a** PAn film in Argon saturated MeOH + $LiClO_4$ + H^+ electrolyte. **b** PAn in N_2 saturated MeOH + $LiClO_4$ + H^+ electrolyte. R_e electrolyte resistance; R_1 pore resistance; Z_{FLW} Finite Length Warburg impedance; R_2 charge transfer resistance of intermediates; CPE_1 constant phase element of the metal/solution double layer capacitance; CPE_2 constant phase element of the film capacitance (polymer/solution depletion layer)

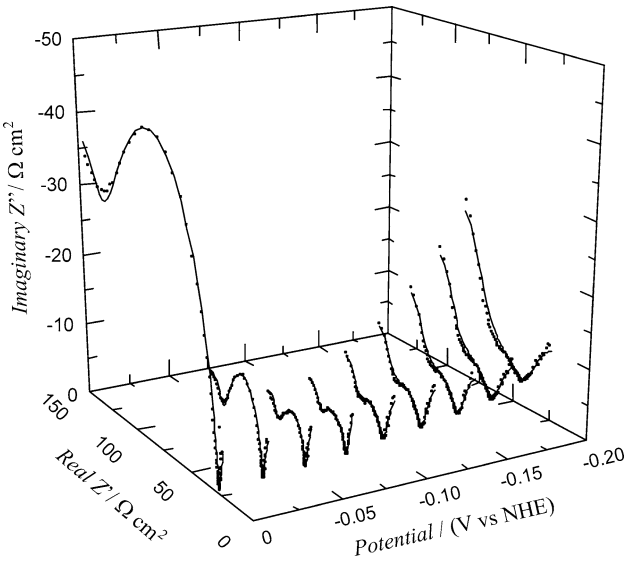

Fig. 4 The ac impedance response of a PAn film depends on the applied potential in MeOH + $LiClO_4$ + H^+. The film thickness was 1.5 μm and the applied pressure was 50 bar N_2

$$Z_{CPE} = \frac{1}{C \cdot (i\omega)^n}\left(i=\sqrt{-1}\right) \text{ And } (\omega = 2\pi f). \quad (1)$$

Depending on the value of n $(-1 < n < 1)$, representing rotation of the complex plane impedance plot, Z_{CPE} might be an inductance $(n = -1)$, a resistance $(n = 0)$ or a Warburg impedance $(n = 1/2)$ [20, 21]. If $n = 1$, then the equation is identical to that of a capacitance. Usually, in an equivalent circuit, a *CPE* is used instead of a capacitor to describe non-homogeneities in a system. These non-homogeneities result from the roughness or porosity of the surface and in such a case, it is expectable that double layer may not behave like a capacitor [24–31].

The second semi-circle describes the charge transfer reaction of intermediates (Fig. 4). In that case, the semi-circle can be characterized as the sum of R_2, CPE_2, and Z_{FLW} and R_2 can be considered as a charge transfer resistance of possible intermediates such as $\bullet N_2H$. The constant phase element CPE_2 describes the capacity of the polymer film (Fig. 2). The Warburg impedance Z_{FLW} added to the circuit with a time constant T_{FLW} states the presence of N_2 in the film. The real part R_{FLW}, describes the transport phenomena of N_2 or intermediates into the polymer film and can be calculated according to Eq. 2.

$$Z_{FLW} = \frac{R_{FLW} \cdot \tanh(i \cdot T_{FLW} \cdot \omega)^{0.5}}{(i \cdot T_{FLW} \cdot \omega)^{0.5}}. \quad (2)$$

If the coating material (polymer film) has the optimum thickness, the low frequencies can penetrate into the bulk phase completely and create a Finite Length Warburg element (Z_{FLW}) with transmissive boundary and the Z_{FLW} value can be calculated with Eq. 2 [26–33]. In Eq. 2 the

Table 1 The fitted data of the EIS measurements on a PAn electrode (40 cycles) in the presence of 0.03 mol/L^{-1} H_2SO_4 in a MeOH + $LiClO_4$ solution under 50 bar N_2 pressure

Potential/V (NHE)	$R_1/\Omega cm^2$	CPE_1		$R_2/\Omega cm^2$	CPE_2		Finite Length Warburg impedance/Z_{FLW}	
		$C_1/\mu F\ s^{n-1}$	n_1		$C_2/mF\ s^{n-1}$	n_2	T_{FLW}/s	$R_{FLW}/\Omega\ cm^2$
0	21.28 (0.19)	0.16 (13.70)	0.87 (1.22)	86.75 (0.73)	0.93 (1.15)	0.89 (0.37)	5.52 (8.46)	82.84 (5.08)
−0.025	22.03 (0.22)	0.22 (13.93)	0.85 (1.27)	29.43 (0.78)	0.90 (2.67)	0.85 (0.67)	3.27 (6.18)	23.47 (3.44)
−0.050	22.63 (0.25)	0.22 (13.41)	0.85 (1.21)	19.76 (1.09)	1.58 (3.96)	0.74 (1.07)	2.86 (5.59)	17.36 (3.02)
−0.075	23.58 (0.29)	0.26 (12.93)	0.84 (1.18)	18.79 (1.58)	3.17 (4.53)	0.63 (1.46)	3.10 (5.83)	17.69 (3.17)
−0.100	26.59 (0.47)	0.86 (14.55)	0.75 (1.46)	19.00 (2.70)	4.56 (6.51)	0.56 (2.45)	3.70 (7.79)	21.71 (4.38)
−0.125	28.04 (0.57)	1.45 (15.04)	0.72 (1.57)	20.37 (3.24)	5.06 (7.10)	0.54 (2.87)	4.23 (8.56)	27.86 (4.93)
−0.150	29.92 (0.76)	2.44 (16.46)	0.68 (1.80)	21.90 (4.17)	5.41 (8.33)	0.51 (3.63)	4.58 (9.26)	35.80(5.43)
−0.175	32.35 (1.16)	3.82 (18.59)	0.65 (2.10)	23.86 (5.68)	5.78 (10.14)	0.47 (4.95)	4.94 (10.11)	45.77 (6.05)
−0.200	34.45 (2.82)	3.95 (25.23)	0.65 (2.77)	28.51 (9.74)	6.44 (13.05)	0.37 (8.78)	5.32 (10.76)	58.35 (6.63)

Data were calculated through equivalent circuit in Fig. 3b

R_e 5 Ωcm^2; n_1, n_2 correlation coefficients; T_{FLW} time constant of the Finite Length Warburg impedance; R_{FLW} resistance of the Finite Length Warburg impedance; () Error ± ratio; R_1 pore resistance; R_2 charge transfer resistance of intermediates

T_{FLW} value is equal to L^2D^{-1} where L is the effective diffusion thickness, and D is the diffusion coefficient.

The calculated kinetic parameters of the PAn-coated Pt electrode under 50 bar N_2 in MeOH + $LiClO_4$ electrolyte is shown in Table 1.

In Table 1, R_e value describes the electrolytic resistance and has a value of *ca.* 5 Ωcm^2. The pore resistance R_1 is the sum of charge transfer resistance and the diffusion layer resistance [24]. At the applied potential range, the charge transfer resistance results from H_{ad} formation on the metal surface. The variation of diffusion layer with applied potential leads to a shifting of pore resistance to higher values. The charge transfer resistance, R_2, in the Nyquist curves changes also with increasing potential in the negative direction. The highest resistance value is obtained at 0.0 V (NHE) and the smallest at −0.075 V. However, the preparative electrolysis was done at −0.12 V (NHE) to keep the current constant [23]. n_1 and n_2 are the parameters of CPE_1 and CPE_2, respectively shown in Eq. 1. The CPE_2 with C_2 defines film capacity. This capacitance is a function of the potential, because the width of the depletion region does also vary with the applied potential. If the applied potential becomes more negative, the depletion region extends and the capacity of the film increases continuously. As the consequence, the time constant value T_{FLW}, arises, which indicates that the diffusion of $N_2/\bullet N_2H$ at potentials from 0.0 to −0.2 V (NHE) becomes more effective in the film($\sqrt{T_{FLW}} \sim L$).

The n_2 values decrease at more negative potentials. This can be explained through the diffusion capacity of the depletion layer; the diffusion character becomes dominant while the capacitive character of the film decreases.

3.3 Interpretation of the impedance spectra of PAn-coated electrodes under N_2 and Ar

In addition, to the above mentioned data with N_2, to characterize and to understand the behaviour of bulk PAn film, the impedance measurements were carried out under Ar atmosphere as well. The impedance response of the electrode under Ar and N_2 atmosphere is shown in Fig. 5.

The first semi-circle describes the metal–solution double layer and it is observable by both of the gases employed. The second semi-circle in the low frequency range may describe the film behaviour. In case of Ar, all pores of the polymer are closed and the resistance in the film becomes higher (Fig. 5). Under dinitrogen atmosphere, the resistance becomes smaller which means, a charge transfer reaction occurs and it is considerable that N_2 molecules are reduced in this region.

Furthermore, it would be interesting to compare the impedance characteristics also of the blank Pt at the same frequency range by employing N_2 and Ar. Nyquist and Bode diagrams of blank Pt and Pt/PAn electrodes at −0.12 V (NHE) are shown in Fig. 6.

In the high frequency range, the pore resistance of blank Pt (Fig. 6, curves 1 and 2) is smaller than that of the PAn-coated Pt electrode (Fig. 6, curve 3). This is an expected result because a coated Pt has more porosity than the blank metal surface. In the low frequency range, the second semi-circle of blank Pt under Ar atmosphere is greater than that under N_2 atmosphere and it is greater than a PAn-coated Pt electrode in the presence of N_2.

In the low frequency range, the charge transfer resistance on PAn-coated platinum is smaller compared to all other

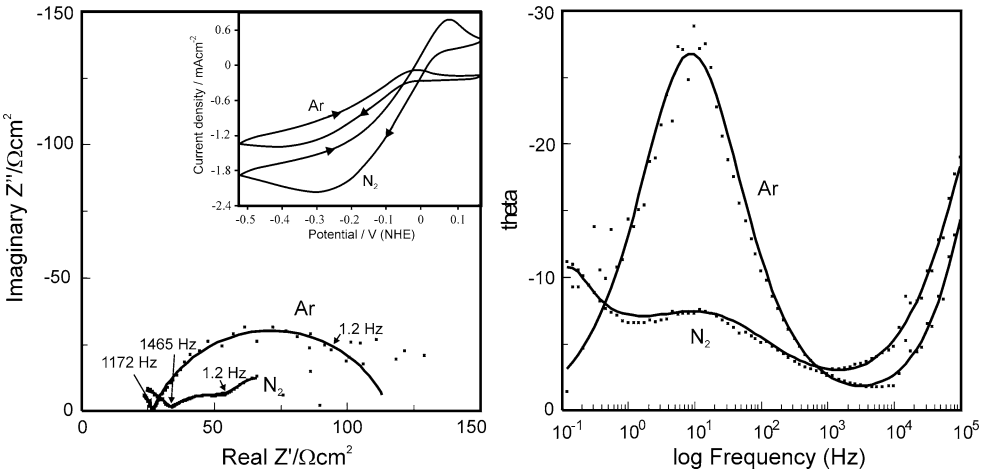

Fig. 5 Complex impedance plots and Bode diagrams of a PAn electrode at −0.12 V (NHE) from 100 kHz to 0.1 Hz in MeOH + $LiClO_4$ + H^+ under 50 bar argon atmosphere and 50 bar N_2 saturated solution. The *solid lines* represent the best fitting results according to the equivalent circuits. *Inset diagram* Cyclic voltammograms of the PAn electrode in MeOH + $LiClO_4$ + H^+, under 50 bar argon atmosphere and saturated (50 bar) with N_2. $v = 5$ mVs^{-1}

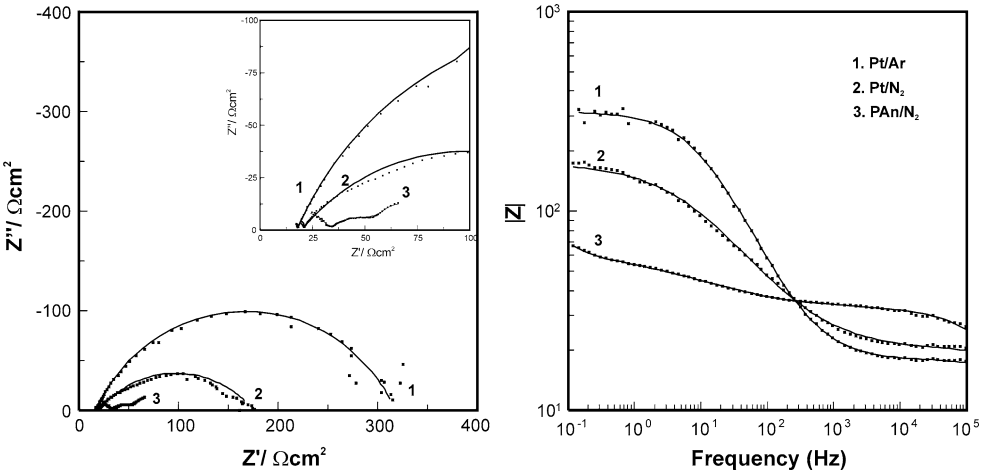

Fig. 6 Nyquist and Bode diagrams of Pt and Pt/PAn electrodes at −0.12 V (NHE) in MeOH + $LiClO_4$ + H^+ and 50 bar Ar and N_2 saturated solution

resistances visible in the curve (in the presence of dinitrogen). This behaviour can only be explained through the presence of intermediates which are formed by hydrogenation of N_2 (for example $\bullet N_2H$). These intermediates can diffuse deep into the pores and the hydrogenation starts on the metal surface. In other words, polymer film act as an adsorption place (mediator) for the intermediates and as a following step, H_{ad} atoms are transferred to the intermediates.

3.4 Dependence on the applied potential

Film capacity CPE_2 and charge transfer resistance R_2 depends on the applied potential. The CPE_2 changes of blank Pt and PAn-coated Pt under different gas atmospheres versus applied potential is shown in Fig. 7.

In the potential range between −0.05 and −0.12 V (NHE) the film capacity changes significantly, if N_2 is available in the solution (Fig. 7). This may indicate that the pores of polymer film contain charged intermediates of the dinitrogen fixation. Under Ar atmosphere, there is no significant increase of the capacity in the same potential range. This fact leads to the conclusion that under Ar atmosphere, there is only a film resistance due to fully filled pores of polymer film by Ar. Under same conditions, the capacity of blank Pt remains constant under Ar as well as N_2 atmosphere.

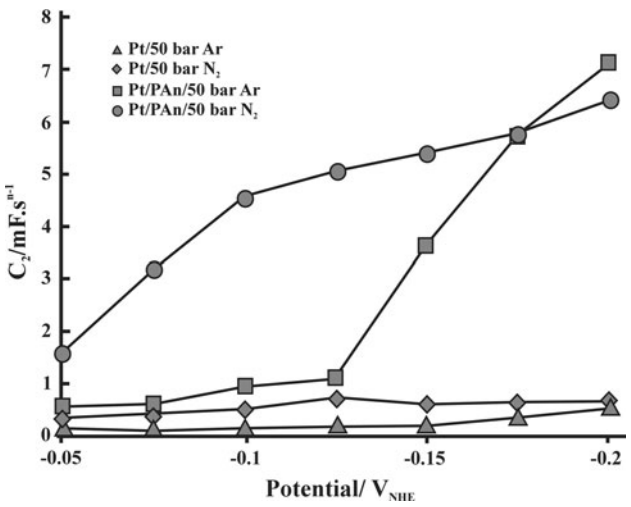

Fig. 7 The change of CPE_2/mF s^{n-1} values with applied potential under 50 bar Ar and 50 bar N_2 atmosphere on blank Pt and on Pt/PAn

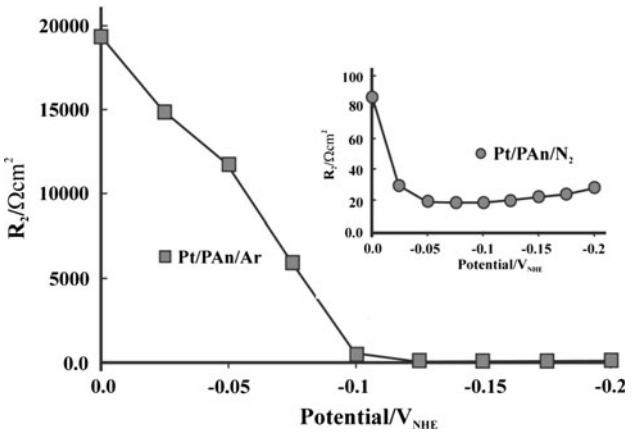

Fig. 8 The change of R_2 resistance of Pt/PAn and Pt electrode with potential under different gas atmospheres

The change of charge transfer resistance, R_2, versus applied potential of PAn-coated Pt is shown in Fig. 8.

Under Ar atmosphere, there is a high film resistance for PAn-coated Pt electrode between 0.0 and −0.1 V (NHE) and it becomes smaller in negative direction (Fig. 8). Dropping of R_2 values indicates a charge transfer reaction on Pt/PAn electrode under N_2 atmosphere (Fig. 8, inset diagram). This reaction does not occur on blank Pt. This fact leads to the conclusion that the hydrogenation reaction of dinitrogen can take place only in the presence of a polymer film on the metal surface. We suppose that the reaction may take place in open pores of polymer film reaching up to metal surface.

3.5 Dependence on the film thickness

The film thickness is one of the most important parameters for the N_2-fixation and has a direct influence on the N_2-reduction which can also be followed by impedance spectroscopy (Fig. 9). Electrochemical impedance spectroscopic investigations reveal also that the film capacitance CPE_2 and R_2 values change with the film thickness as well (Table 2). The lowest R_2 value of *ca.* 20.3 Ωcm^2 has been obtained by 40 cycles.

Experimentally, we found out that a polymer film obtained after 40 cycles gave best product yields and this appears the optimum film thickness. According to the calculation of Johnson et al. [19, 27–33], 40 cycles are equivalent to 1.5 ± 0.3 μm. With the knowledge of film thickness and by using the T_{FLW} value from Table 1, a diffusion coefficient of $(5 \pm 2)\times10^{-9}$ cm^2 s^{-1} was calculated.

3.6 Dependence on the applied pressure

During the dinitrogen reduction, also the R_2 and CPE_2 values in the Nyquist curves change with varying pressure.

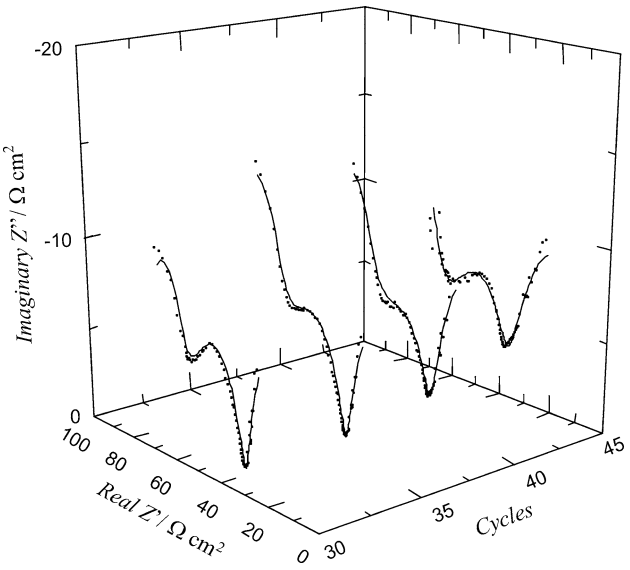

Fig. 9 Complex impedance plots of a PAn electrode depending on the film thickness at −0.12 V (NHE) from 100 kHz to 0.1 Hz in MeOH + $LiClO_4$ + H^+ solution under 50 bar N_2 atmosphere. The *solid lines* represent the best fitting results according to the equivalent circuit in Fig. 2b

Under 50 bar N_2 atmosphere, the resistance R_2 reaches a minimum. At lower pressures (20 and 40 bar), the R_2 values are higher than those at 50 bar and with increasing pressure, the R_2 (at 60 and 80 bar) becomes higher again (Fig. 10).

The dropping of the resistance R_2 from 20 to 50 bar (optimum value) can be explained through the increasing solubility of the N_2 in the electrolyte solution. At higher values than 50 bars, the R_2 values arises again because of the (T_{FLW} value decreases again) hindered H_{ad} formation at this pressure value. Consequently, the reaction rate of hydrogen evolution becomes lower by exceeding optimum pressure values. The fitting results of the EIS measurements depending on the applied pressure are presented in Table 3.

3.7 Kinetical and mechanical aspects

The parameters obtained through the Nyquist curves under N_2 and Ar atmospheres were used for further kinetic calculations. The sum of R_1 and R_2 is called polarization resistance and the plot of $-\log(R_{pol})$ versus applied potential is called EIS–Tafel curve; its slope can be considered as equal to Tafel slope [34]. In order to compare the results obtained by the EIS measurements, we recorded also Tafel curves under same experimental conditions (Fig. 11).

The EIS–Tafel curves and Tafel plots (Fig. 11, inset diagram) have similar course in the same potential range (0; −0.05 V). When we consider the curves obtained under N_2 atmosphere in EIS–Tafel diagram and in Tafel plots, the slopes are almost identical with 122 and 123 mV/dec,

Table 2 The fitted data of the EIS measurements on a PAn electrode with different number of cycles in the presence of 0.03 mol L^{-1} H_2SO_4 in MeOH + $LiClO_4$ under 50 bar N_2 pressure at −0.12 V (NHE)

Number of cycles	R_1/Ωcm^2	CPE_1		R_2/Ωcm^2	CPE_2		Finite Length Warburg impedance/Z_{FLW}	
		C_1/μF s^{n-1}	n_1		C_2/mF s^{n-1}	n_2	T_{FLW}/s	R_{FLW}/Ωcm^2
30	23.79 (0.49)	0.86 (18.93)	0.75 (1.91)	22.02 (1.86)	1.99 (5.92)	0.65 (1.80)	2.77 (6.20)	23.05 (3.40)
35	24.38 (0.45)	1.21 (16.54)	0.73 (1.72)	22.14 (2.20)	3.55 (5.41)	0.61 (1.92)	3.94 (7.01)	30.10 (3.99)
40	28.04 (0.57)	1.45 (15.04)	0.72 (1.57)	20.37 (3.24)	5.06 (7.10)	0.54 (2.87)	4.23 (8.56)	27.86 (4.93)
45	31.43 (1.09)	4.60 (17.80)	0.65 (2.03)	25.6 (4.56)	3.14 (9.96)	0.54 (3.96)	11.16 (283.92)	29.34 (145.54)

Data were calculated through equivalent circuit in Fig. 3b

R_e 5 Ωcm^2; n_1, n_2 correlation coefficients; T_{FLW} time constant of the Finite Length Warburg impedance; R_{FLW} resistance of the Finite Length Warburg impedance; () Error ± ratio; R_1 pore resistance; R_2 charge transfer resistance of intermediates

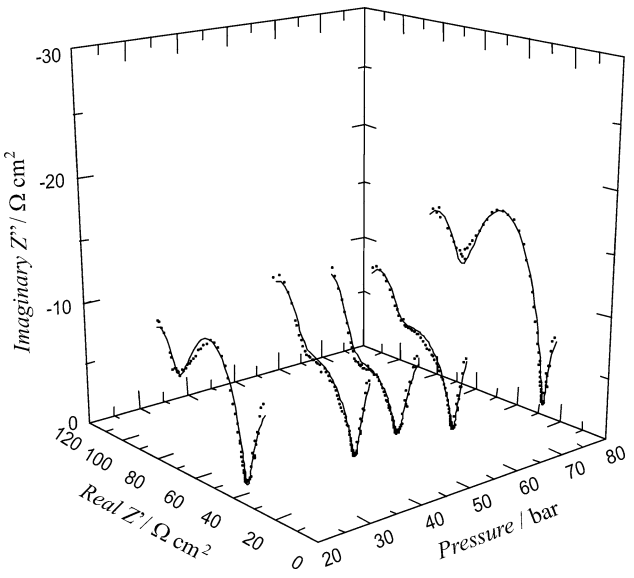

Fig. 10 Nyquist plots of a PAn electrode changing with applied pressure at −0.12 V (NHE) from 100 kHz to 0.1 Hz in N_2 saturated MeOH + $LiClO_4$ + H^+ solution

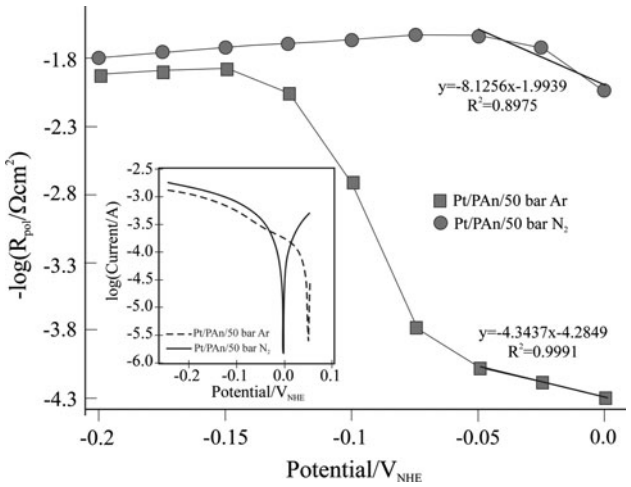

Fig. 11 log (R_{pol})-Potential curves of the PAn electrode in Ar and N_2 saturated MeOH + $LiClO_4$ + H^+ solution. *Inset diagram* Tafel plots of the PAn electrode with the same conditions

respectively. In the case of Ar atmosphere the slope gives almost twice higher values of *ca.* 230 mV/dec. By considering the value of 122 mV/dec, a direct electron transfer from electrode to the N_2 molecule is not viable in this potential range between 0 and −0.05 V. But, this potential range and 122 mV slope values are for an electron transfer for a H_{ad} formation (Volmer reaction) under our conditions. After the formation of H_{ad}, the hydrogenation of N_2 molecules to ammonia occurs.

For the mechanism of electrochemical hydrogenations, there are three possible paths:

i. Volmer reaction:

$$M + H_3O^+ + e \leftrightarrow MH_{ad} + H_2O$$

This is a direct electron transfer reaction to a H^+ and under ideal conditions it has a Tafel slope of 118 mV/dec.

ii. Heyrovsky reaction:

$$MH_{ad} + H_3O^+ + e \rightarrow M + H_2 + H_2O$$

This is a combined mechanism. In the first step an electron transfer occurs to a H^+ and then two H_{ad} recombines to H_2.

iii. Tafel reaction:

$$MH_{ad} + MH_{ad} \rightarrow 2M + H_2$$

This is a chemical recombination reaction [35].

Through the data resulting from EIS and Tafel curves, we can say that the electrochemical hydrogenation of N_2 to NH_3 corresponds to a Tafel slope of 122 mV/dec very well. In that case the rate-determining step must be the Volmer reaction. However, if Ar was employed, the slope with 230 mV/dec is almost two times higher than those under N_2 atmosphere. This leads to conclusion that it can only be a H_{ad} recombination reaction under Ar atmosphere.

We propose a mechanism in which dinitrogen was adsorbed on the polymer modified surface and these leads to path 1. The electrochemical step for the electroreduction

Table 3 The fitted data of the EIS measurements on a PAn electrode (40 cycles) in the presence of 0.03 mol L^{-1} H_2SO_4 in MeOH + $LiClO_4$ at −0.12 V (NHE) under different N_2 pressure obtained by using equivalent circuit in Fig. 3b

Pressure/bar	$R_1/\Omega cm^2$	CPE_1		$R_2/\Omega cm^2$	CPE_2		Finite Length Warburg impedance/Z_{FLW}	
		$C_1/\mu F\ s^{n-1}$	n_1		$C_2/mF\ s^{n-1}$	n_2	T_{FLW}/s	$R_{FLW}/\Omega cm^2$
20	27.97 (0.48)	2.20 (16.52)	0.69 (1.83)	31.55 (1.74)	1.38 (5.24)	0.74 (1.54)	3.29 (11.07)	23.35 (6.07)
40	25.28 (0.45)	0.48 (15.57)	0.79 (1.48)	24.96 (3.14)	5.21 (5.64)	0.54 (2.25)	3.20 (6.29)	26.37 (3.55)
50	28.04 (0.57)	1.45 (15.04)	0.72 (1.57)	20.37 (3.24)	5.06 (7.10)	0.54 (2.87)	4.23 (8.56)	27.86 (4.93)
60	23.80 (0.39)	0.29 (15.87)	0.83 (1.45)	25.76 (2.59)	4.22 (4.96)	0.58 (1.84)	2.72 (5.58)	24.20 (3.12)
80	23.20 (0.26)	0.34 (15.08)	0.82 (1.42)	36.17 (1.03)	0.98 (2.88)	0.84 (0.77)	2.72 (5.37)	31.59 (2.85)

R_e 5 Ωcm^2; n_1, n_2 correlation coefficients; T_{FLW} time constant of the Finite Length Warburg impedance; R_{FLW} resistance of the Finite Length Warburg impedance; () Error ± ratio; R_1 pore resistance; R_2 charge transfer resistance of intermediates

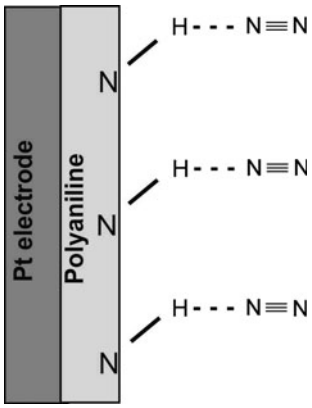

Fig. 12 The proposed reaction mechanism for the ammonia formation through the N_2 fixation on a Pt/PAn electrode (schematically)

is the formation of H_{ad}. With the addition of a H_{ad} to N_2, the species in step 2 is formed and further H_{ad} transfers lead to ammonia (path 3).

$$H_3O^+ + e \rightarrow H_{ad} + H_2O \quad (I)$$

$$N_2 + H_{ad} \rightarrow N_2H_{ad} \quad (II)$$

$$N_2H_{ad} + 5H_{ad} \rightarrow 2NH_3 \quad (III)$$

The proposed mechanism in Fig. 12 is plausible due to the low overpotential applied in our studies [23]. A direct electron transfer onto dinitrogen molecule can not be possible at these potential values due high energy demand of this molecule. That is why, the reduction of dinitrogen occurs via H_{ad} atoms which are evoluted in the polymer/Pt depletion layer.

From the slope of EIS–Tafel and Tafel curves, the transfer coefficient α can be calculated by Tafel equation [34].

$$\eta = a - b \log R_{pol} - \log R_{pol} \approx \log\ j \quad (3)$$

$$a = 2.303\ RT/(\alpha nF) \text{ and } b = -2.303\ RT/(\alpha nF)$$

By using Eq. 3 we calculated α value of 0.48.

The exchange current density of the reaction j_0, can be calculated from Eq. 4.

$$j_0 = RT/nFR_{ct}. \quad (4)$$

In the equation n is the number of transferred electrons, $R(= 8.314\ J/K\ mol)$ is the gas constant, $F(= 96487\ C/mol)$ is the Faraday constant and R_{ct} is the total charge transfer resistance which can be calculated from linear regression in Fig. 11. The calculated j_o value is 2.6×10^{-4} A cm^{-2}.

Summarized the calculated kinetic parameters from Tafel curves and EIS–Tafel plots from Eqs. 3 and 4 are shown in Table 4.

4 Conclusion

The N_2 fixation was studied on a PAn-coated Pt electrode at an extremely low overpotential value of −0.12 V. The mechanism of the reduction was investigated via Electrochemical Impedance Spectroscopy under high pressure. It was found out that the reduction of dinitrogen obeys a Volmer type hydrogenation reaction. H_{ad} atoms formed electrochemically are transferred to N_2 and the intermediates are formed. In that process, polymer films act as an

Table 4 The calculated kinetic parameters from Tafel curves and EIS–Tafel plots

	Tafel			EIS–Tafel		
	$j_0/A\ cm^{-2}$	α	b (slope) (mV)	$j_0/A\ cm^{-2}$	α	b (slope) (mV)
Pt/PAn/50 bar N_2	1.81×10^{-4}	0.48	122	2.6×10^{-4}	0.48	123
Pt/PAn/50 bar Ar	1.02×10^{-4}	0.26	228	1.33×10^{-6}	0.26	230

adsorption place (mediator) for N_2 and for the intermediates.

Further parameters such as film thickness and pressure which influence the electroreduction of N_2 to NH_3 are also investigated. The optimum polymer film thickness was determined to be 1.5 μm and optimum pressure 50 bar. The diffusion coefficient of dinitrogen has a value of $(5 \pm 2)\times 10^{-9}$ cm^2 s^{-1} in such a polymer/platinum system. Transfer coefficient α, is found to be 0.48 and the exchange current density j_o, is found to be 2.6×10^{-4} A cm^{-2}.

Acknowledgments We wish to give our thanks to DFG (Deutsche Forschungsgemeinschaft) and TUBITAK (National Research Foundation of Turkey) for financial support of this work. We also wish to give our thanks to Prof. Dr. Mehmet ERBİL (Cukurova University, Department of Chemistry, Turkey) for his helpful explanations about impedance behaviours of polymer coated metals.

References

1. Mussini PR, Mussini T (2002) Pure Appl Chem 74:593
2. Hidai M, Mizobe Y (1995) Chem Rev 95:1115
3. Sellmann D, Fürsattel A (1999) Angew Chem Int Ed 38:2023
4. Schrauzer GN, Guth TD (1977) J Am Chem Soc 99:7189
5. Tsuneto A, Kudo A, Sakata T (1994) J Electroanal Chem 367:183
6. Gavrilov AB, Strelets VV, Pospíšil L (1990) J Electroanal Chem 289:117
7. Tsuneto A, Kudo A, Sakata T (1993) Chem Lett Jpn 5:851
8. Cook RL, Sammells F (1988) Catal Lett 1:345
9. Kordali V, Kyriacou G, Lambrou Ch (2000) Chem Commun 17:1673–1674
10. Pospíšil L, Bulíčková J, Hromadová M, Gál M, Civiš S, Cihelka J, Tarábek (2007) J Chem Commun 22:2270–2272
11. Musiani MM (1990) Electrochim Acta 35:1665
12. Roßberg K, Paasch G, Dunsch L, Ludwig S (1998) J Electroanal Chem 443:49
13. Pasquali M, Pistoia G, Rosati R (1993) Synth Met 58:1
14. Glarum SH, Marshall JH (1987) J Electrochem Soc 134:142
15. Chen WC, Wen TC, Gopalan A (2002) Synth Met 128:179
16. Rubinstein I, Sabatani E (1987) J Electrochem Soc 134:3078
17. Fiordiponti P, Pistoia G (1989) Electrochim Acta 34:215
18. Hu CC, Chu CH (2001) J Electroanal Chem 503:105
19. Johnson BJ, Park SM (1996) J Electrochem Soc 143:1269
20. Chen WC, Wen TC, Hu CC, Gopalan A (2002) Electrochim Acta 47:1305
21. Grzeszczuk M (1994) Electrochim Acta 39:1809
22. Köleli F, Röpke T, Hamann CH (2003) Electrochim Acta 48:1595
23. Köleli F, Röpke T (2006) Appl Catal B Environ 62:306
24. Tüken T, Erbil M, Yazici B (2007) Conducting polymers and corrosion protection. In: Wang IS (ed) Corrosion research trends. Nova Science Publisher Inc., Hauppauge, pp 275–316. ISBN 978-1-60021-733-3
25. Hitz C, Lasia A (2001) J Electroanal Chem 500:213
26. Hoshino K, Inui M, Kitamura T, Kokado H (2000) Angew Chem 112:2558
27. Bell J, Dunford AJ, Hollis E, Henderson RA (2003) Angew Chem Int Ed 42:1149
28. Le Grand N, Muir KW, Pétillon FY, Pickett CJ, Schollhammer P, Talarmin J (2002) Chem Eur J 8:3115
29. Reiher M, Hess BA (2002) Chem Eur J 8:5332
30. Shaver MP, Fryzuk MD (2003) Adv Synth Catal 345:1061
31. Rusina O, Linnek O, Eremenko A, Kirsch H (2003) Chem Eur J 9:561
32. Bazhenova TA, Shilov AE (1995) Coord Chem Rev 144:73
33. MacDonald JR, Johnson WB (1987) In: MacDonald JR (ed) Impedance spectroscopy: emphasizing solid materials and systems, Wiley-VCH, New York
34. Damian A, Omanovic S (2006) J Power Sources 158:464
35. Aydın R, Köleli F (2006) Prog Org Coat 56:76